

## DETAILED QUANTITATIVE SEQUENCE STRATIGRAPHIC INTERPRETATION FOR THE CHARACTERIZATION OF AMANGI FIELD USING SEISMIC DATA AND WELL LOGS

<sup>1</sup>Inichinbia, S. and <sup>2</sup>Halidu Hamza

<sup>1</sup>Department of Physics, University of Port Harcourt, Choba, Port Harcourt, Nigeria

<sup>2</sup>Department of Geology, Ahmadu Bello University, Zaria, Nigeria

Email: [sonny.inichinbia@yahoo.com](mailto:sonny.inichinbia@yahoo.com) , [sonny.inichinbia@uniport.edu.ng](mailto:sonny.inichinbia@uniport.edu.ng)

Phone: +234(0)7030087653

*Received: 22-09-2020*

*Accepted: 30-09-2020*

### ABSTRACT

*The sequence stratigraphy of Amangi field of the Niger Delta was studied using seismic data and well logs. The field is a structurally complex one and presents serious challenges to hydrocarbon exploration and production. The main objective of these analyses is to identify sand intervals using the available data. Well log data were used as additional tools to constrain the seismic correlations in order to solve the correlation problem. The well logs were evaluated for the field's petrophysical properties by combining the gamma ray and resistivity logs to determine reservoir zones with considerable hydrocarbon saturation. Also, the relationship between some basic rock properties/attributes and litho-types were determined for the study area. Next, well-to-seismic ties were produced and two horizons were picked. Acoustic impedance inversion was also performed which revealed "hard sands" due to mixed lithologies (heterolithics). This made it difficult to discriminate the sands from shales in the P-impedance domain alone. So, progress was made to determine the net-to-gross of the field. The analysis revealed that these reservoirs have shaly sand with shale content of 10%, porosity averaging 21%, and hydrocarbon saturation of 90%. The result established a vertical stack of a series of reservoirs in an anticlinal structure of which the H1000 and H4000 stand out for their huge volumes of rich gas condensate accumulation. This discovery provoked the drive for the first phase of development of this field.*

**Keywords:** stratigraphy, facies, net-to-gross, horizon, lithology, well-to-seismic tie, impedance

### INTRODUCTION

The field was discovered by well-002 which was drilled in 1992 after an initially 2D seismic survey that same year which was reprocessed in 2005. But because of some unresolved challenges, between 2008 and 2010 a new 3D seismic data was acquired with long offset cable and high fold of coverage, and processed in 2011 which provided a better resolution and structural interpretation across the reservoirs of

interest (Inichinbia *et al.*, 2014a). A detailed quantitative lithostratigraphic interpretation of Amangi field, an onshore Niger Delta field was conducted on well log and 3D seismic data sets. This formation exhibits complex geological variations which make exploration and development a challenge. Reservoir geometry and internal architecture in the Niger Delta can vary over short distances with rapid lateral and vertical changes in lithology and porosity. Understanding such variations is critical to

designing an optimum development strategy for prospects in this basin.

Reservoir characterization focuses on estimating subsurface physical properties of rock units which are important in hydrocarbon exploration and exploitation. Such properties include lithology, porosity, saturation, and permeability. Although these properties are frequently measured in wells penetrating such rock units, the data obtained are local and sparse, as economics necessitates that wells be few and far between (Contreras *et al.*, 2020; Pendrel & Schouten, 2020; Webb *et al.*, 2020; Aminu & Olorunniwo, 2011). Reliably predicting lithologic and saturation heterogeneities is one of the key problems in reservoir characterization. Sources of reservoir heterogeneity include variations in lithology, porosity, pore fluid properties, etc. They control not only the amount of hydrocarbons that may be present, but also their recoverability from distributed reservoir compartments (Contreras *et al.*, 2020; Mukerji *et al.*, 1998). A consistent sequence stratigraphic framework is necessary for mapping depositional systems especially in structurally complex areas (Aminu & Olorunniwo, 2011) like this field under study. This study is aimed at unraveling the details of litho-fluid facies variation in Amangi field. The objectives of this work include facies prediction, reservoir characterization, prospect delineation, identification of sand intervals to develop the sequence stratigraphic framework and depositional system for the field under study using well logs and seismic amplitude variation with offset (AVO/AVA) data.

### **Location and Geology of the Study Area**

The field is located within Licence OML 21, in the northeastern corner of the OML 21 licence, 70 km northwest of Port Harcourt in the greater Ughelli depobelt of the Niger Delta as shown in Figure 1. The field measures about 12 km by 5 km and was discovered by Well-002 which was drilled in 1992. It consists of alternating units of sandstone and shale, which makes it the major petroleum bearing stratigraphic unit. The formation consists of siliciclastics of 2,500 m thick and accumulated in delta front, and fluvio-deltaic environments (Short & Stauble, 1967). The age of the producing sand intervals of this formation ranges from Eocene to Pliocene and becomes progressively younger southward. Detailed knowledge of the Niger Delta was obtained from the works of Short & Stauble (1967), Tuttle *et al.*, (1997), Nwachukwu and Chukwura (1986), Amogu *et al.* (2011) & Bustin (1988).

The structure of Amangi field is a complex collapsed crest, rollover anticline, predominantly shore face and channel deposits with distinctive coarsening upward characteristics. Hydrocarbons in the field are found between 7,300 feet subsea (ftss) and 12,600 ftss in a predominantly deltaic sequence consisting of alternating sands, silts and shale layers (Tuttle *et al.*, 1999; Omudu *et al.*, 2008). Six wells have penetrated the H1000 reservoir in the field and only three wells have penetrated the H4000 reservoir. The location of the wells on the field is displayed in Figure 2 and the logs from these wells are displayed in Table 1.

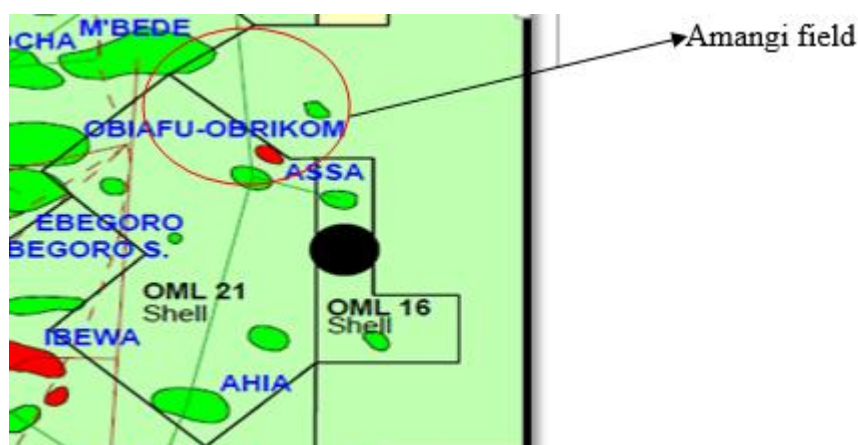


Figure 1. Map of the Niger Delta showing the study area. The encircled portion is the location of Amangi field.

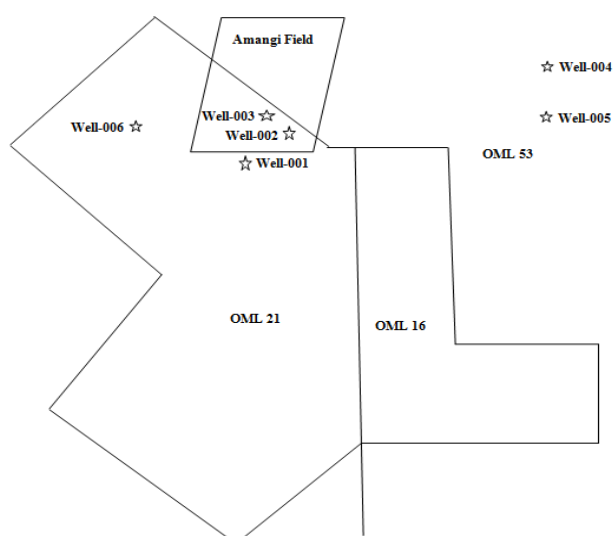


Figure 2. Schematic diagram of the study area showing the locations of the wells used in this study. Four out of a total of six wells are located in OML 21 whereas the rest two wells are sited in OML 53 (After Inichinbia *et al.*, 2014b).

## MATERIALS AND METHOD

Materials used in this work include anisotropic 3D seismic data (full and three partial angle stacks), well data, interpreted horizons and industry proprietary softwares such as Jason Geoscience Workbench, Rokdoc, Petrel version 2.0, ArcGis, and Techlog. The data for this study were obtained solely from field investigations by the SPDC of Nigeria Ltd.

## Seismics

The seismic methodology is an already established one consists of characterizing each portion of a trace over the reservoir interval by a series of seismic attributes. The principle involves automatically analyzing the character of the seismic traces at the reservoir level and relating or tying the variations to geological variations of the reservoirs. The attributes used to characterize the traces were computed from the series of the reflection coefficient

amplitudes (from the inversion) of the 200 ms window above and below the H1000 and H4000 horizons (Contreras *et al.*, 2020; Goodway *et al.*, 1997; Li *et al.*, 2000; Samantaray & Gupta, 2008; Castagna *et al.*, 1985; Fatti *et al.*, 1994 and Bachrach & Gofer, 2020).

Several seismic attributes were integrated to improve the prediction of the reservoir properties and the horizons are clearly displayed in Figure 3.

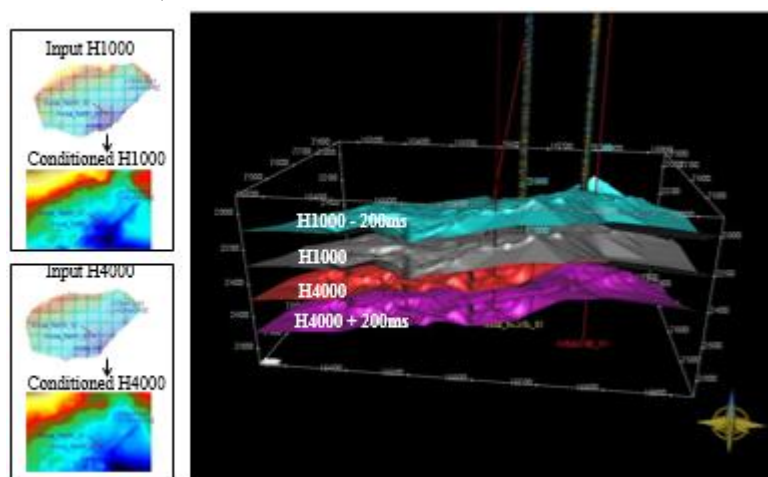


Figure 3. Input and conditioned H1000 and H4000 horizons with 200 ms window above and below the horizons.

### Well logs

Well log data were acquired from the drilled appraisal wells in the field. Prerequisites such as log editing, conditioning, timing and log calibration, well tie location, seismic bandwidth and S/N ratio, quality control of both the seismic and well logs and

the use of well tie diagnostics were performed and all play an important part in making close well ties (Simm & White, 2002; White & Simm, 2003; White, 1997; Goodway *et al.*, 1997; Li *et al.*, 2000; Samantaray & Gupta, 2008; Castagna *et al.*, 1985; Fatti *et al.*, 1994).

Table 1. Some wells in Amangi Field showing suite of logs in each well. Only Well-002 has a complete suite of good quality logs in the area, needed for this work (After Inichinbia *et al.*, 2014c).

Well	Gamma ray (API)	Calliper (inches)	Resistivity ( $\Omega$ m)	Density ( $\text{g}/\text{cm}^3$ )	Sonic ( $\mu\text{s}/\text{ft}$ )	Pressure (psi)	Formation inflow test	Checkshot (ms)
Well-001	YES	YES	YES	NO	YES	NO	NO	YES
Well-002	YES	YES	YES	YES	YES	YES	YES	YES
Well-003	YES	YES	YES	YES	YES	YES	NO	NO
Well-004	YES	YES	YES	YES	YES	NO	NO	NO
Well-005	YES	YES	YES	YES	YES	NO	NO	NO



correlations existed, a statistical relationship was built to convert the seismic information into the related properties at each trace location (Fournier *et al.*, 2002). In this present work, the correlation analysis was carried out in the vicinity of wells where both geologic and seismic information are available. Estimates of lithology, porosity, and saturation were then made from geologic, well log, and seismic data.

The resolutions of the seismic reflection follow gross bedding and as such they approximate time lines. The key is that the contrast represented by seismic lines comes from bedding surface and not lateral variation (facies changes). The structure of Amangi field is an elongated rollover

anticline bounded to the south and southeast by large boundary faults that throw down towards the south and southeast. Towards the north is a regional growth fault that joins with the northeastern boundary fault to close the structure towards the east. It is a fault dip closure against a large growth fault which separates it from a neighbouring field. The H4000 hydrocarbons are trapped in a closure against the southern and southeastern faults. The structure is bounded to the south and to the southwest by large faults that throw down towards the south and southeast. The western aquifer part of the structure is not covered by the 3D seismic data, but the fact that the reservoirs are overpressured suggests another bounding fault there (see Figure 5).

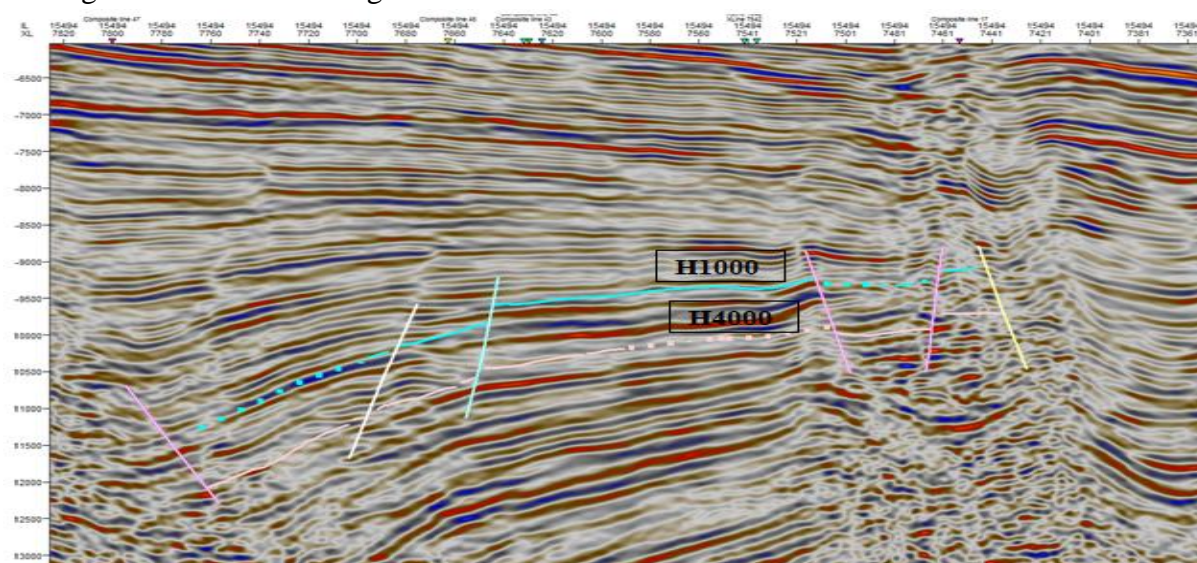


Figure 5. Seismic section of the structure of Amangi field showing the distribution of faults in the study area. The markers indicate the interpreted seismic horizons (H1000 and H4000 tops).

Faults were picked on vertical sections along the direction of maximum transport. Subsequently, the fault sticks were modelled to produce the corresponding fault surfaces. Horizon interpretation constituted the second phase of the interpretation. The mapped events were identified from well correlation and tying well tops to seismic

events. Horizons were picked on laterally continuous reflections, starting from the well locations. The petrophysical analysis for all the wells in the study area shows the difficulty of lithological discrimination by acoustic impedance from the wells (see Figure 6).

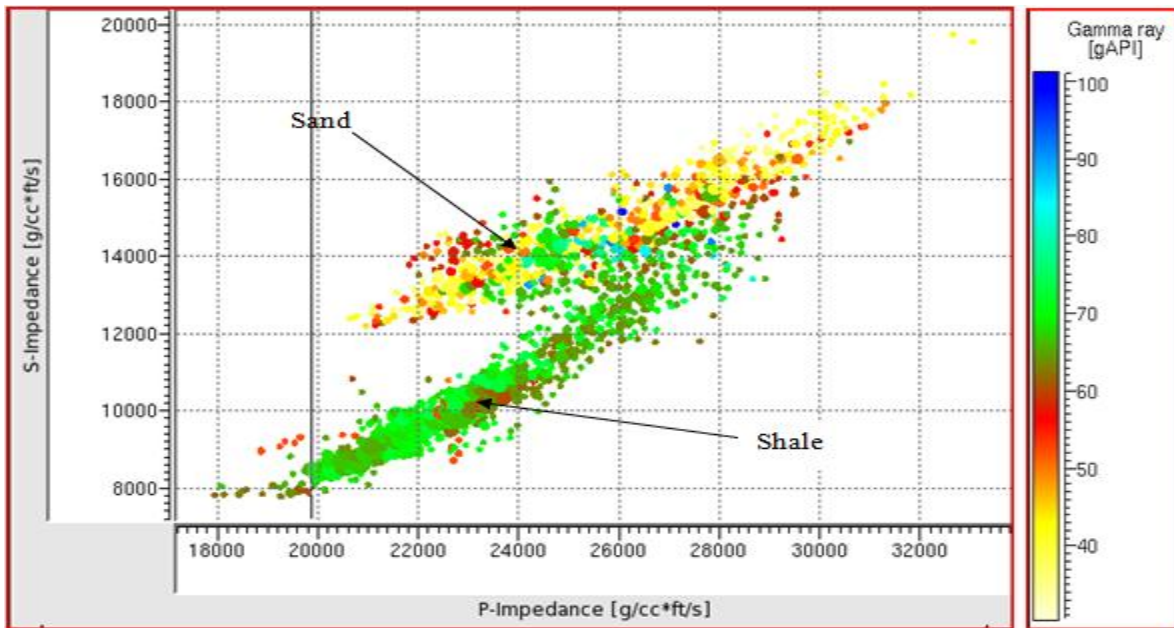


Figure 6. Well P-impedance versus S-impedance colour coded to gamma ray. P-impedance alone could not discriminate between sand and shale, except in the S-impedance domain.

Hence, rock physics analysis used the combination of computed porosity from density log against acoustic impedance from the transformation of the seismic reflectivities and density and porosity

against compressional velocity colour coded to gamma ray values. These analyses allowed separation of sand and shale facies as demonstrated in Figure 7.

Figure 7 shows the newly processed anisotropic prestack depth migrated (PreSDM), 3D seismic data of the survey area displayed in (a) variable density and (b) wiggle trace. The horizons indicating the top of the reservoirs is displayed and gamma ray log is superimposed on them for quick identification of the litho-facies (Bachrach & Gofer, 2020).

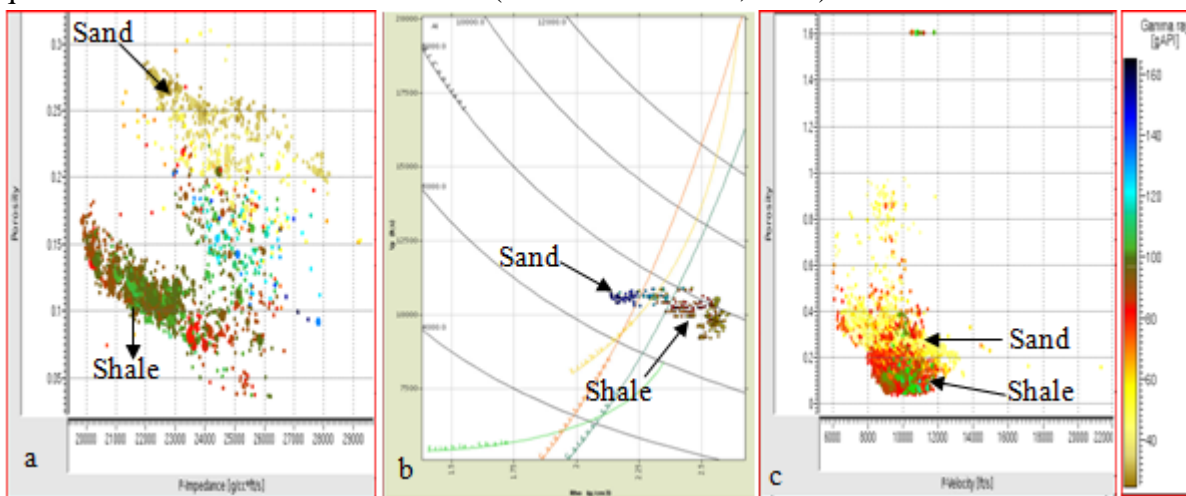


Figure 7. Well crossplots of (a) porosity versus P-impedance (b) compressional velocity versus bulk density and (c) porosity against P-velocity colour coded to gamma ray.

Seismic facies of the H1000 top show a trough while that of the H4000 shows a peak (Figure 8).

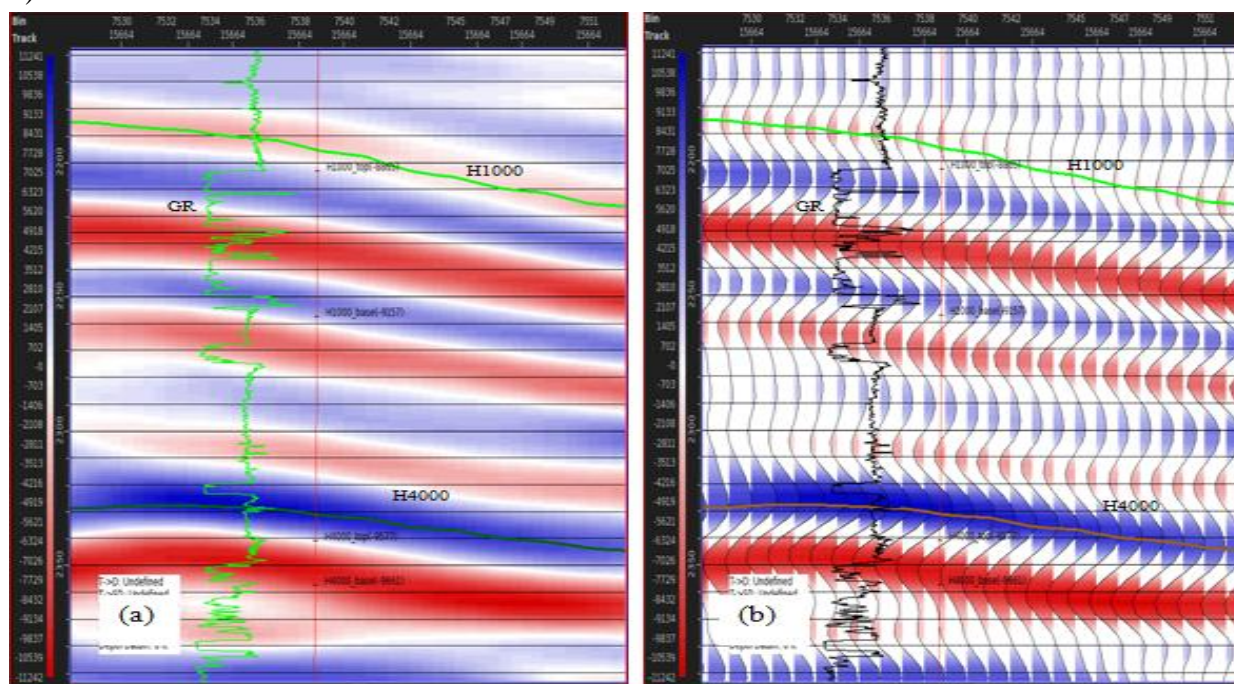


Figure 8. The newly processed anisotropic PreSDM 3D seismic data of the survey area shown in (a) variable density and (b) wiggle trace. Displayed on the seismic volumes are the loops indicating the reservoirs (H1000 and H4000) being studied, gamma ray log and the depths to the tops and base of the reservoirs (After Inichinbia *et al.*, 2014c).

There is good reflection quality and continuity in the full stack seismic section. However, amplitude changes that could be related to porosity are not apparent because the changes in velocities over a small zone are smoothed by the propagating wavelet. The H1000 shows a thick section of sandstones with intercalations of shale as shown by the gamma ray log superimposed on the sections. The H4000 has lesser sand packages compared to the H1000. However, geological information is introduced to guide the seismic facies analysis. This makes clear the sand distribution within the reservoir region with clean reservoir sands interspaced with shaly sands. These shaly sand units could serve to compartmentalize the reservoir and act as flow barriers to hydrocarbon present.

A detailed lithostratigraphic interpretation of seismic data was attempted, which was aimed at defining the lateral variations of the H1000 and H4000 reservoirs in Figures 9, 10 and 13. Well-006 reaches its target depth above the H4000 and the reservoir is completely faulted out in Well-001 (Figures 9, 10 and 13). The formation is a complex series of continental (deltaic) siliciclastics consisting of Tertiary sands and shales in sequence. At the crest of the field, well-001 targeting shallower reservoirs in the hanging wall of the bounding fault intersected the bounding fault and penetrated Amangi field. It also encountered a Gas Down To (GDT) in the H1000, while the H4000 was faulted out (Figures 10, 12 and 14). Well-002 encountered a GDT in the H1000 reservoir

and a Gas Water Contact (GWC) in the H4000, and yielded high quality pressure data across a wide depth range, and pressure, volume, temperature (PVT) samples from both H1000 and H4000 (Figures 11, 12 and 14). The reservoirs were found to be overpressured by some 2000 psi (approximately 0.66 psi/ft). Well-003 encountered an Oil Water Contact (OWC) at the same depths as seen in the two adjacent wells (Well-004 and Well-005 drilled by Chevron Nigeria Ltd) in the OML 53 (Figures 12 and 14). Well-006 encountered the H1000 reservoir in the

aquifer but did not reach the H4000 reservoir as shown in Figures 11 and 14.

H1000 is interpreted as a series of amalgamated channel packages and the sand units of blocky log character are interpreted to represent thick amalgamated channel sands. The general absence of shoreface units at their base is due to erosion by these channel packages. This is supported by the thickness of the channel packages. The sand units of more variable log character are interpreted to represent shoreface sands.

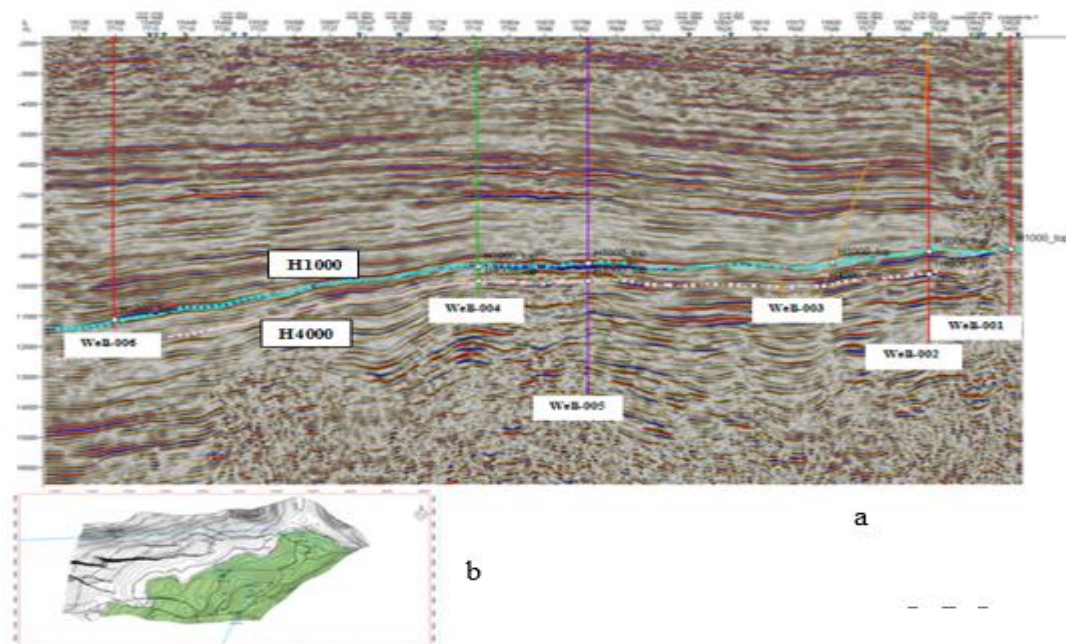


Figure 9a and b. The newly processed prestack depth migrated (PreSDM) 3D seismic volume superimposed with the horizons in dotted lines H1000 and H4000 and the six wells drilled on the field (Inichinbia *et al.*, 2014c). The blue line in the depth structure contour map shows how the displayed seismic section was extracted from a 3D volume passing between six wells (well-006 through well-001) in the gas and brine legs.

To the west of the reservoir, all the H1000 reservoir units decrease in quality and are interpreted as shoreface sands. Figures 11, 12 and 14 show a subregional correlation of major sands of the field and reveals the H1000 sands to be laterally extensive and they maintain a similar (good) log profile

away to some 14 km south of the field. H1000 hydrocarbons are trapped in a closure against the southern and southeastern faults. The crest is in the southeastern corner at approximately 2,590.80 m (8500 ft), The H1000 reservoir dips towards the northwest, with a dip of

some 3.5° across the hydrocarbon filled area, and steeper in the aquifer. Through the anisotropic 3D seismic data, the detailed delineation of the structure became improved by better imaging in the crestal areas at the southeastern and southern edges of the field, in the shadow zone of the large boundary faults (Figure 10).

The H4000 sands are interpreted to represent a series of channelized shoreface deposits (where channels are fluvial-dominated). In H4200 a thick channel is interpreted as a tidal channel at Well-002 but as a more fluvial dominated channel in Well-005 (to the east) and at Well-003 (to the west of the field). In the H4000 there are three internal correlatable flooding surfaces separating four parasequences. The character of each parasequence varies from well to well and facies correlation is more complicated than in the H1000 reservoir (Figures 12 and 14). Overall the shoreface packages are preserved better than in the H1000 but they do not exist at every well for every reservoir unit. In general, each parasequence displays shale, overlain by a coarsening up profile that passes upwards into a blocky, fining upward profile. The coarsening upward successions are interpreted to represent shoreface deposits while the blocky to fining upward successions are interpreted to represent channel deposits.

From well to well the amount of shoreface deposits in each parasequence varies due to the localization of channels, which erode underlying deposits in a nonuniform manner. The quality and type of channel varies from well to well. Most channel sands are thought to be fluvial dominated except the H4200 in Well-002 where the channel is tidally dominated. Here the

channel is very heterogeneous with sand and shale inter-beds but this passes laterally into fluvial dominated channels in Well-005 (to the east) and Well-003 (to the west). H4000 closure residing in the foot wall side of the southern and southeastern boundary faults. From Figures 10, 12 and 14, three wells penetrate H4000, but gas was detected only by Well-002. Well-005 is water bearing and Well-004 has an Oil Water Contact (OWC).

Six main genetic facies are identified: marine shale, lower shoreface, upper shoreface, tidal channel, channel fill and channel heterolithics. These were determined from electro-facies analysis of the density and from gamma ray and neutron-density logs. Effective porosity and water saturation were also available. The effective porosity was averaged over the reservoir sections. We decided to focus on the effective porosity and the litho-facies proportions, because both types of information were considered important for constraining any geologic model with seismic derived information. The marine shales are highly correlatable and variable in thickness. These shales are characterized by high neutron-density separation, coupled with low resistivity and high gamma ray. They are generally laterally extensive except where channel incision has occurred. Typical indicators from sidewall samples included the presence of shell fragments and calcareous compositions.

Figure 11 displays the H1000 reservoir as seen by all the six wells in the study area. The proximal (upper) part of the field has higher sandstone content than the distal (lower) part, hence, well-006 met the H1000 in the aquifer.

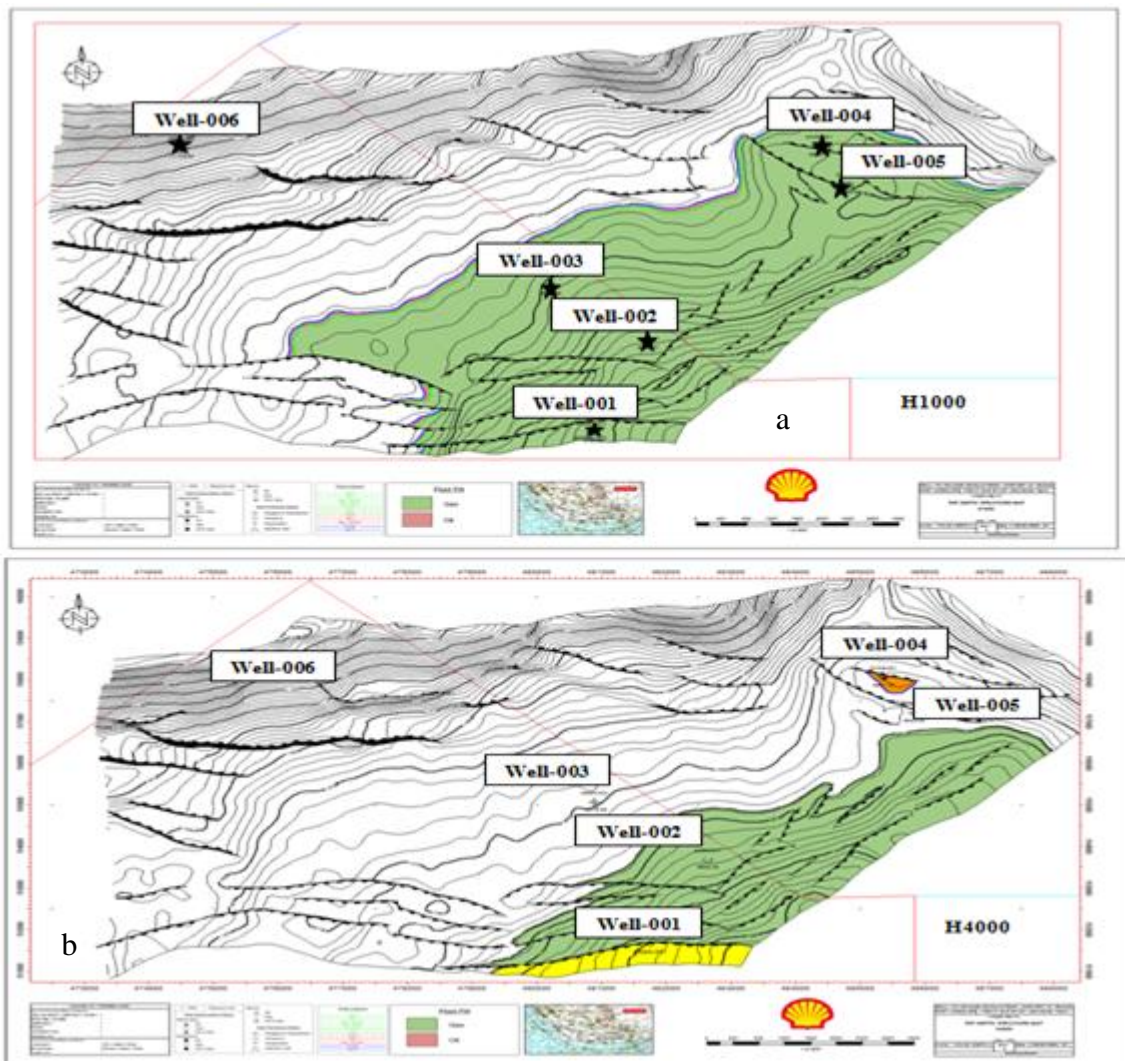


Figure 10a and b. Depth structure contour maps of the tops of the gas reservoir sandstones (H1000 (a) and H4000 (b)) respectively, as interpreted from the 3D seismic data. Contour interval is 50 m. The locations of seismic lines (in red) across the structure are indicated. The shaded areas (in green) are proven hydrocarbon saturated areas. The structure also shows some major faults and drilled wells in the study area (After Inichinbia *et al.*, 2014c).

Thus, the field consists of a stacked sequence of reservoirs in shore-face and channel deposits. Five wells encountered nine hydrocarbon bearing reservoirs between 2,286 m and 3,352.80 m (7,500 ft and 11,000 ft). These are the E1000, E2000, E9000, E9500, H1000, H2000, H3000, H4000 and H5000 (Figure 13). Among

these, two reservoirs stand out for their volumes: the H1000 and the H4000 with a rich gas condensate accumulation. The H1000 is the largest reservoir. Together, the H1000 and H4000 drive and define the field development plan (FDP), and the FDP is focused on them.

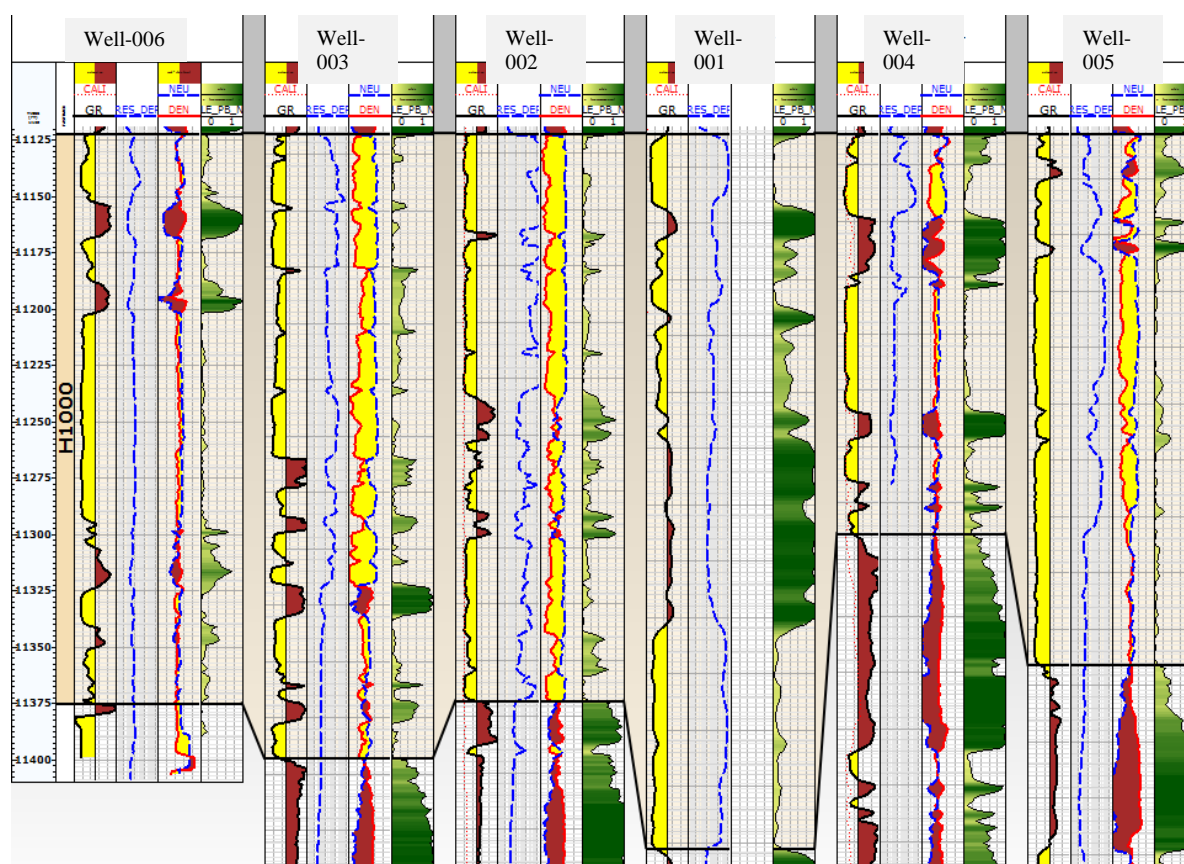


Figure 11. The log types displayed are, gamma ray, caliper, resistivity and neutron-density.

The structure is bounded to the south and to the southwest by large faults that throw down towards the south to southeast. At H1000 level, the field measures some 12 km long and 5 km wide. The crest is in the southeastern corner at approximately 2,438.40 m (8500 ft), and the hydrocarbon-water-contact at 2,875.78 m (9435 ft TVDSS) yields a column of some 289.56 m (950 ft). The distance between Well-002 and the adjacent wells (Well-004 and Well-005) is 5 km. The reservoir dips towards the northwest, with a dip of some  $3.5^\circ$  across the hydrocarbon saturated area (shaded green in Figure 10).

The E-sands are deposited within a thick shale package and are dominated by incised pro-grading shore-face deposits. The H-sands are thicker sands comprised of more stacked channel sand deposits with some estuarine influences and tidal channel deposits. The E2000 and H1000 reservoirs are separated by a regional shale package several thousand feet thick that hampers effective dewatering of the underlying sediments, and controls the onset of overpressures. The shallower E1000 and E2000 sands are hydrostatically pressured, while the underlying H-reservoirs are overpressured (see Figure 12).

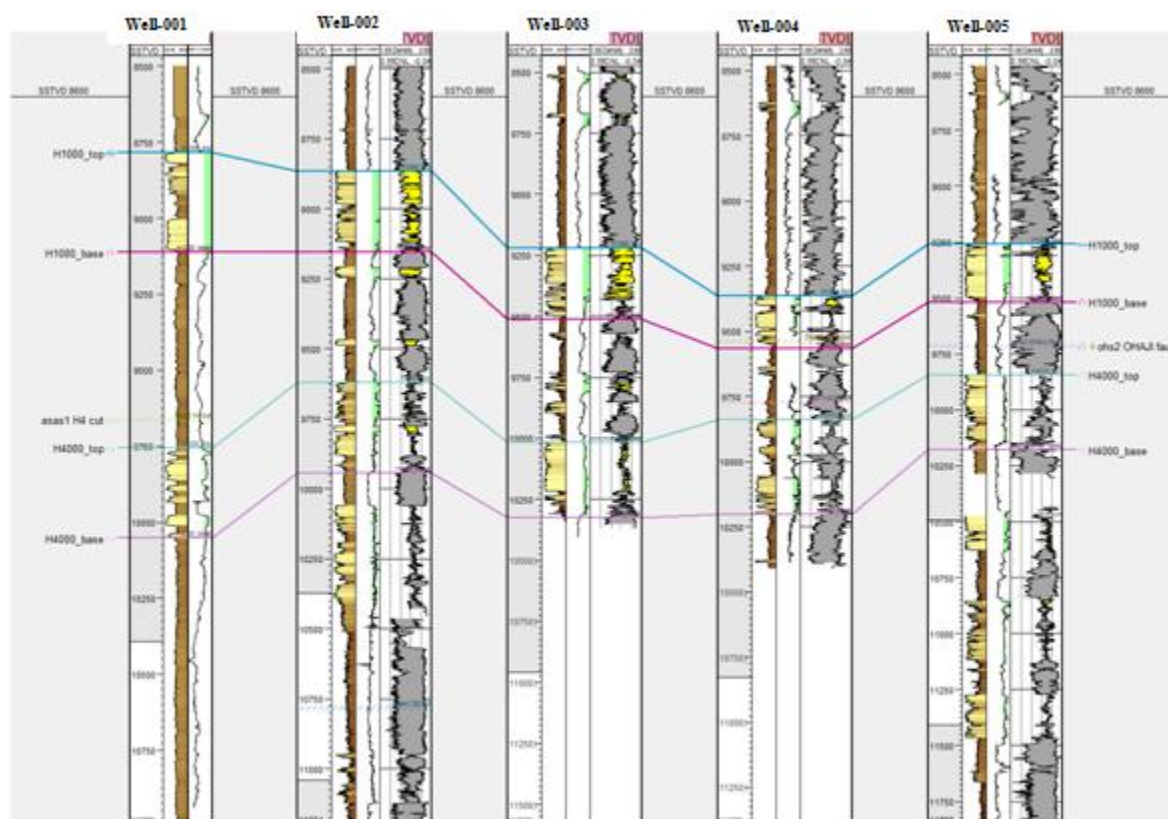


Figure 12. Well sections showing the hydrocarbon saturated intervals denoted as reservoirs H1000 and H4000 as delineated on the well logs. Five wells were used in the delineation and the log types were resistivity, gamma ray, calliper and neutron-density logs.

Overall, the H1000 - H5000 sequence comprises a sand-rich package, which is likely to share a common aquifer. At H1000 level, these wells define a clear hydrocarbon-water-contact (HCWC). Within the Amangi field the sands are seen to be laterally continuous with a slight thickening to the north due to syn-sedimentary activity on the growth fault just north of the Well-006. Here, the H1000 and H4000 sands are correlated at higher resolution using sequence stratigraphic interpretations between the six wells in the field area.

Generally the sediments represent fluvio-deltaic deposits recording a series of relative sea level fall followed by flooding. The H1000 sands contain four system tracts dominated by amalgamated channel packages. There is little or no shore-face remaining in the upper tracts where channels have eroded into the underlying shale units. The H4000 sands contain four system tracts where shore-face to channel progradations are preserved.

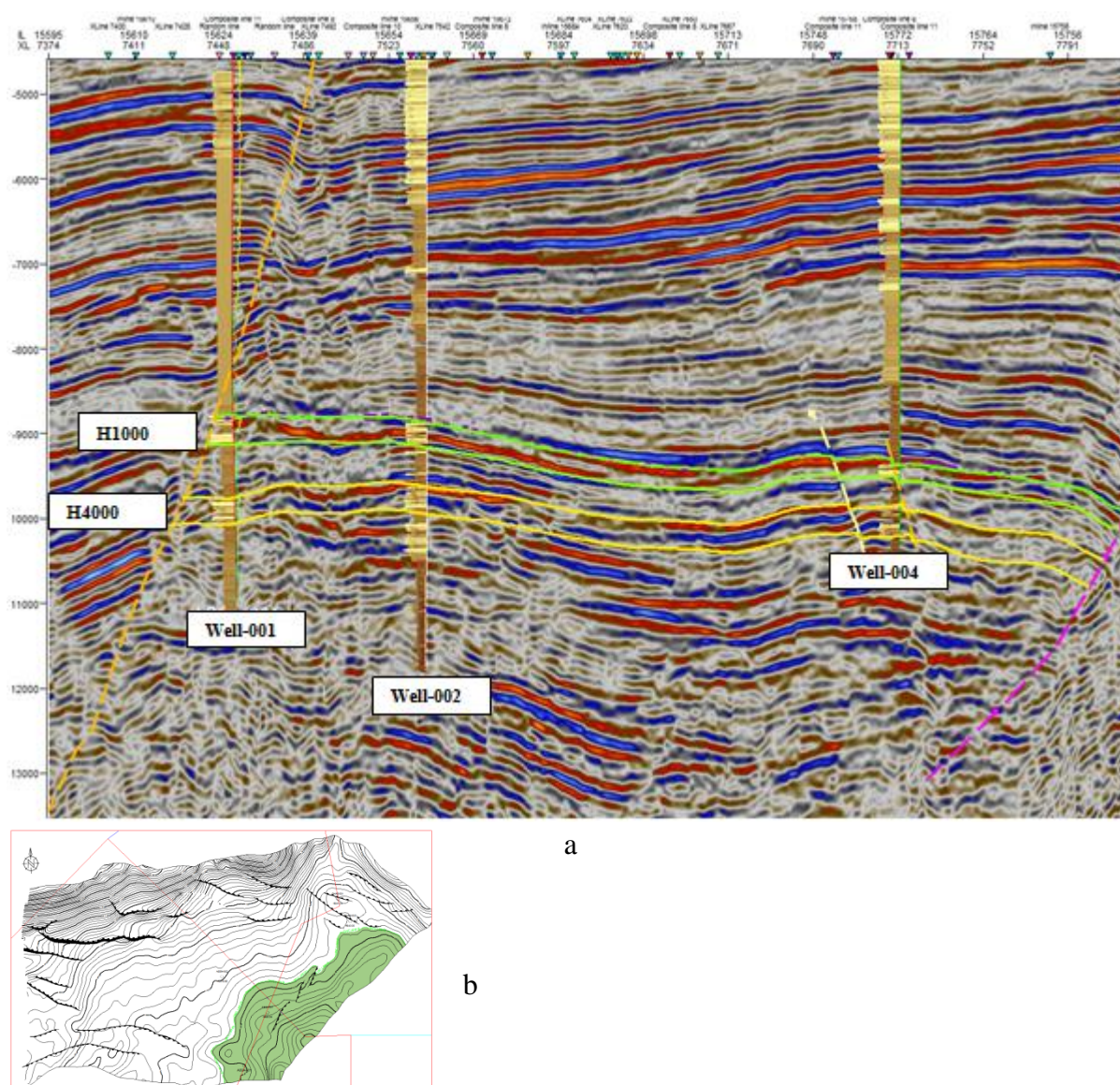


Figure 13a and b. Seismic section superimposed with gamma ray logs of well-001, well-002 and well-004 showing the reservoir intervals. The green horizontal markers indicate H1000 and the yellow horizontal markers denote H4000 (courtesy: SPDC, of Nigeria Ltd). The red lines in the depth structure contour map shows how the displayed seismic section was extracted from 3D volume passing between three wells (well-001, well-002 and well-004) in the gas and brine legs.

Sands and shales thicken to the north (Well-001 to Well-006) due to syn-sedimentary activity on the growth fault at the northern part of the field. Sediment influx is from the north.

#### **Amangi field well-to-seismic tie**

A good well-to-seismic tie exercise was carried out in this work, using the near, mid

and far sub-stack volumes of the new anisotropic 3D seismic data. Every seismic interpretation project needs to begin with an attempt to tie seismic reflectors to geologic units via synthetic seismograms. The first goal in working with the seismic data was to ensure that the borehole seismic and the surface seismic at the borehole trajectory look as similar as possible.

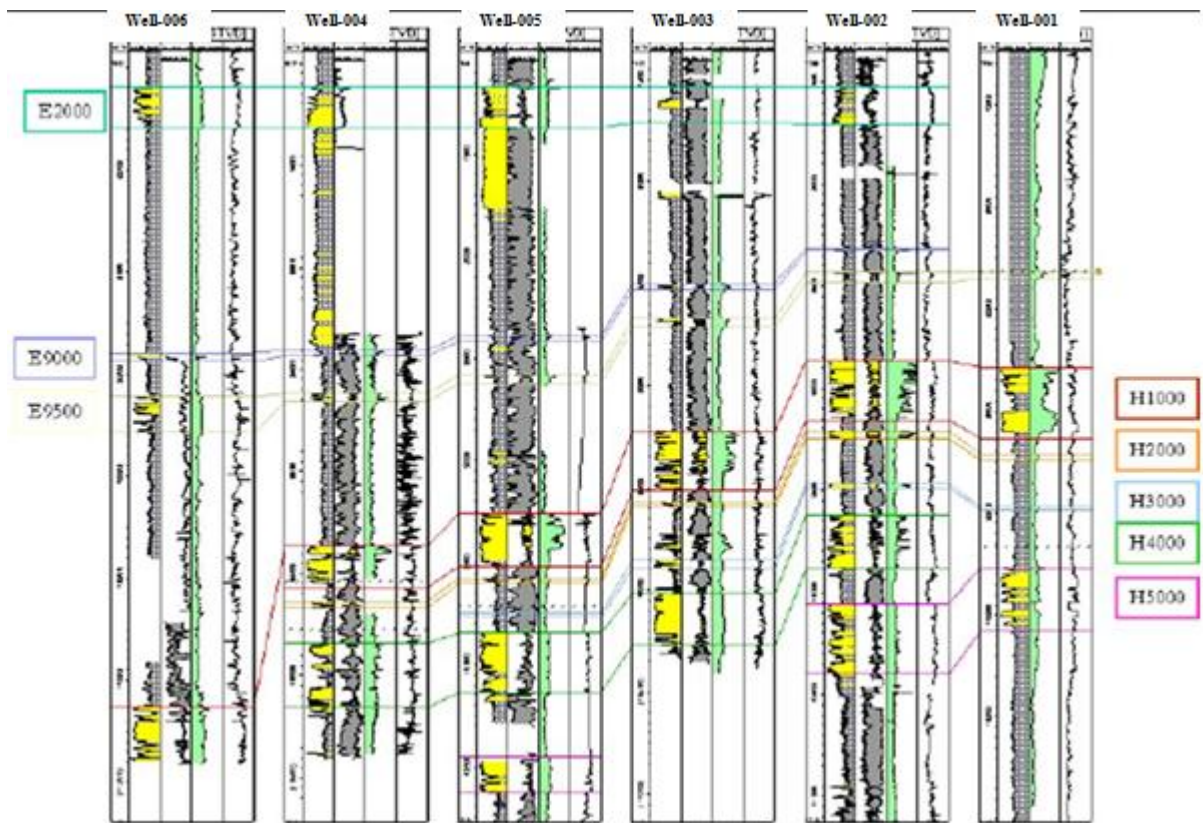


Figure 14. Panel showing a sub-regional correlation of the six appraisal wells drilled in the area of study. The panel also shows some of the major hydrocarbon saturated intervals or reservoirs in the field. Well-006 encountered H1000 in the aquifer.

This achieved, we then tightly link the surface seismic to events at the borehole and subsequently correlated structures and evaluated properties between wells. The seismic data near each well were fitted by iteratively convolving the P-wave impedance logs with the near angle wavelet estimate (Figure 15) to produce the synthetic predicted traces.

The synthetic seismograms agreed very well with the seismic data. The wavelet at each well were found to be very similar, zero phase and the data bandwidth was 10 – 60 Hz as shown in the extreme left panel of Figure 15. The real seismic is shown in the first panel close to the wavelet whereas the synthetic seismogram is in the panel immediately after the actual seismic. The next panel contains the correlation and tops

that also show the horizons under consideration. This correlation shows the degree of agreement between the seismic and the synthetic. The next panel following displayed the P-impedance obtained from the simultaneous inversion of the surface seismic data, overlain by the P-impedance obtained by inverting the seismic data measured at the well. This also showed a good match. A panel labelled drift shows the degree of stretching and/or squeezing. Finally, the panel on the extreme right displayed the gamma ray, P-sonic and P-impedance logs extracted from the inverted P-impedance. This panel also displays the reservoirs of interest in depth (TVDSS). The well was almost vertical and mildly over-pressured (0.6 psi/ft). At the H1000 level, the work resulted in a confident tie at Well-002, Well-003, Well-004, Well-005

and at Well-006. At Well-004, the synthetic seismogram was tied to the seismic and is compatible with a field wide horizon interpretation. At Well-002, the base of the H4000 was confidently tied, but the local match at the top of the H4000 is poor. Well-006 does not penetrate the H4000. The H1000 has a good well-to-seismic tie at Well-002, which defined where the top and base of the H1000 fall on the seismic, with the assumption of a roughly constant H1000 thickness. The base case scenario was depicted by the blue picks, following the top and base of the blue-red doublet, which suggests thinning (pinchout) towards the northeastern part of the field. But at Well-004, there is a significant H1000 thickness again, which means the H1000 has to thicken in the direct vicinity of the well, possibly across a major fault in the area. The seismic-to-well tie of the top of the H4000 is slightly poor at both Well-004 and Well-002. Using the better constrained H1000 top

and H4000 base seismic-to-well ties as analogue, the H4000 top/base case pick was defined to be at the zero crossing, from a soft to hard interface. The pick uncertainty increases in areas of poor seismic resolution; particularly in the middle of the field, northwards towards areas of growth faulting and around the fault shadow zones. The estimated wavelet amplitude and phase spectra and the well-to-seismic tie are shown for Well-002 and Well-004, in Figure 15.

From the well-to-seismic tie we were able to determine the wavelets for the inversion of the seismic reflection data into impedance data. The results of the acoustic impedance inversion and subsequent determination of net-to-gross showed the sand distribution as displayed in Figure 16. The net-to-gross volume is superimposed with the logs of the wells and the target horizons.

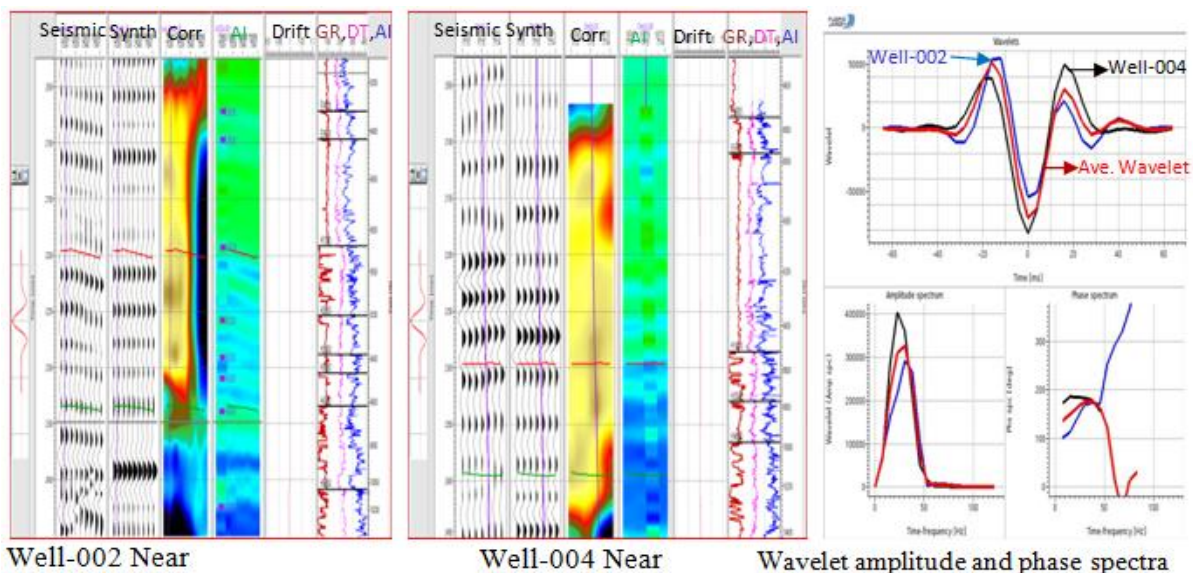


Figure 15. Well-to-seismic ties for Well-002 and Well-004 with horizons and gamma ray, P-sonic and P-impedance logs and wavelet amplitude, phase and spectra. There is reasonable tie between synthetic and seismic data with a cross correlation factor of 0.7 for Well-002 (After Inichinbia *et al.*, 2014c).

The seismic studies also predicted average reservoir properties and seismic facies analysis led to a qualitative geologic interpretation of the seismic character,

highlighting the major reservoir variations which are often related to depositional environment changes (Contreras *et al.*, 2020; Pendrel & Schouten, 2020).

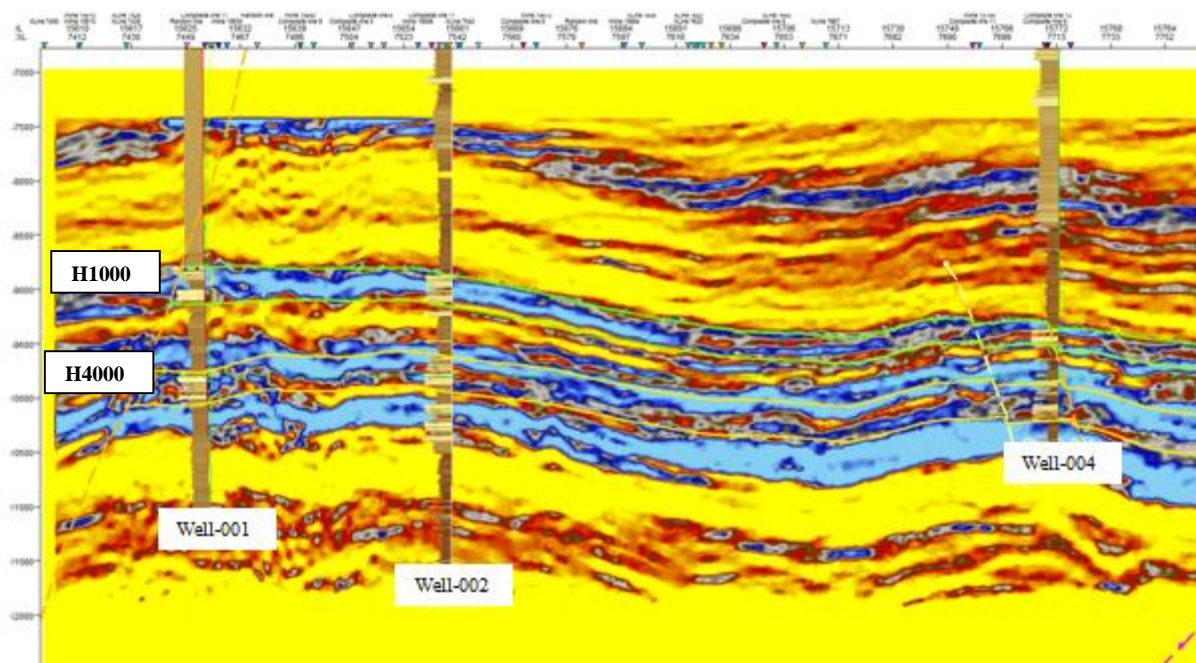


Figure 16. Net-to-gross volume superimposed with gamma ray logs of well-001, well-002 and well-004 showing the reservoir intervals.

## CONCLUSIONS

Lithostratigraphic interpretation of seismic and well data sets covering Amangi field reservoir formations has enabled us to map the sandstone distribution and characterize the average porosity of the formation. The field's sediments comprise a series of sand and shale successions that have been deposited during different relative sea level changes. These sediments have characteristic coarsening upward, fining upward, and blocky and serrated gamma ray/self potential log profiles.

Sandstone distribution was predicted through facies identification and interpretation with well information coupled with seismic information. Based on the well logs and some sidewall samples descriptions, six (6) major facies were identified. These facies are lower shore-

face, upper shore-face, tidal channels, channel fill, channel heterolithics and marine shale. This work demonstrated that seismic data can contribute much to the description of the reservoir variations laterally between the wells.

These represent a gradual transition from clean sandstones to pure shale. The log motifs show fine details of lithologic variation both within the reservoir region and beyond. It delineated a subsurface geologic situation typical of the Niger Delta with numerous meandering sand filled channels and point bars in the southwest, north, and west of the field. The channels cross the study area generally in an east-west direction and possess shale volumes in the range of 8–10%. The gamma ray log values and patterns, and velocity and density logs were used primarily to

determine the different facies with contrasting seismic properties.

Channels in the western region demonstrate good lateral continuity while those in the eastern region are less continuous. This is likely the result of the considerably steeper dips on the western arm of the anticlinal structure which results in an overall southwestward (seaward) dip of the horizon. This shows details of sand distribution within the reservoir region with clean reservoir sands interspaced with silty sands. These silty sand units could serve to compartmentalize the reservoir and act as flow barriers to hydrocarbons. Thus, additional appraisal data, provided by future H1000 and H4000 development wells will be required to mature these reservoirs for future phase developments.

The upper part has higher sandstone content than the lower part, demonstrating the progressive seaward advance of the Niger Delta through geological time. The hydrocarbon bearing interval of Amangi field is part of a succession of Tertiary proximal deltaic deposits separated by laterally extensive shale/shaly heterolithic packages that represent flooding episodes. The sand packages are progradational units that progress upwards from medium quality shoreface into good quality channel units. Laterally extensive channel cuts are filled by a combination of coarse braided fluvial sands, localized delta top shale, and finer shore-face deposits interlayered with thin marine shale. The depositional direction is interpreted to be from north to south.

### **Acknowledgements**

The authors express many thanks to Shell Petroleum Development Company (SPDC) of Nigeria Limited, Port Harcourt for

permission to publish these results. We also thank the geosolution and QI asset teams of the company for their immense assistance and contributions to make this work a success.

### **REFERENCES**

- Aminu, M.B., and Olorunniwo, M.A. (2011) *Reservoir characterization and paleo-stratigraphic imaging over Okari Field, Niger Delta, using neural networks. The Leading Edge, 30(6), 650 – 655.*
- Amogu, D.K., Filbrandt, J. Ladipo, K.O., Anowai, C., and Onuoha, K. (2011) *Seismic Interpretation, Structural Analysis, and Fractal Study of the Greater Ughelli Depobelt, Niger Delta Basin, Nigeria. The Leading Edge, 30(6), 640 – 648.*
- Bachrach, R. and Gofer, E. (2020) *A nonlinear and anisotropic data-driven litho-petroelastic inversion for single-loop subsurface characterization: Theory, uncertainties, and a case study. The Leading Edge, 39(2), 119 – 127.*
- Bui, H. Graham, J. Singh, K.S., Snyder, F., and Smith, M. (2011) *Incorporation of geology with rock physics enables subsalt poststack inversion: A case study in the Gulf of Mexico. Geophysics. 76(5), WB53–WB65.*
- Bustin, R.M. (1988) *Sedimentology and characteristics of dispersed organic matter in Tertiary Niger Delta: origin of source rocks in a deltaic environment. American Association of Petroleum Geologists. Bulletin. 72(3), 277 – 298.*
- Castagna, J.P., Batzle, M.L. and Eastwood, R.L. (1985) *Relationships between compressional-wave and shear-wave*

- velocities in elastic silicate rocks, *Geophysics*, **50**(4), 571-581.
- Contreras, A., Gerhardt, A., Spaans, P. and Docherty, M. (2020) *Characterization of fluvio-deltaic gas reservoirs through AVA deterministic, stochastic, and wave-equation-based seismic inversion: A case study from the Carnarvon Basin, Western Australia. The Leading Edge*, **39**(2), 92 – 101.
- Fatti, J.L., Smith, G.C., Vail, P.J., Strauss, P.J. and Levitt, P.R. (1994) *Detection of gas in sandstone reservoirs using AVO analysis: A 3D seismic case history using the geostack technique. Geophysics*, **59**(9), 1362 – 1376.
- Fournier, F., Dequizez, P.Y., Macrides, C.G., and Rademakers, M. (2002) *Quantitative lithostratigraphic interpretation of seismic data for characterization of the Unayzah Formation in central Saudi Arabia. Geophys.* **67**(5), 1372 – 1381.
- Goodway, B., Chen, T. and Downton, J. (1997) *Improved AVO fluid detection and lithology discrimination using Lamé petrophysical parameters: " $\lambda\rho$ ", " $\mu\rho$ " and " $\lambda/\mu$  fluid stack", from P and S inversions, Canadian Society of Exploration Geophysicists Recorder*, 3– 5.
- Inichinbia, S., Sule, P.O., Ahmed, A.L. and Hamza, H. (2014a) *AVO inversion and Lateral prediction of reservoir properties of Amangi hydrocarbon field of the Niger Delta area of Nigeria. IOSR Journal of Applied Geology and Geophysics*. **2**(2), 08-17.
- Inichinbia, S., Sule, P.O., Ahmed, A.L., and Hamza, H. (2014d) *Modelling the seismic responses of Amangi hydrocarbon field using Gassmann fluid substitution. IOSR Journal of Applied Geology and Geophysics*. **2**(2): 106 – 114.
- Inichinbia, S., Sule, P.O., Ahmed, A.L., and Hamza, H. (2014c) *Well-to-seismic tie of Amangi hydrocarbon field of the Niger Delta of Nigeria. IOSR J. of Applied Geology and Geophysics*. **2**(2), 97 – 105.
- Inichinbia, S., Sule, P.O., Ahmed, A.L., Hamza, H. and Lawal, K.M. (2014b) *Petrophysical analysis of among hydrocarbon field fluid and lithofacies using Well Log Data. IOSR Journal of Applied Geology and Geophysics*, **2**(2): 86 – 96.
- Li, Y., Hunt, L. and Downton, J. (2000) *Sensitivity of rock properties in AVO analysis and prospect evaluation, Society of Exploration Geophysicists, Expanded Abstracts*, 1 – 4.
- Mukerji, T., Jorstad, A., Mavko, G., and Granli, J.R. (1998) *Applying statistical rock physics and seismic inversions to map lithofacies and pore fluid probabilities in a North Sea reservoir. 68<sup>th</sup> Annual Meeting, Society of Exploration Geophysicists, Expanded Abstracts*. 1 – 4.
- Nwachukwu, J.I., and Chukwura, P.I. (1986) *Organic matter of Agbada Formation, Niger Delta, Nigeria. American Association of Petroleum Geologists. Bulletin*. **70**(1), 48 – 55.
- Omudu, L.M., Ebeniro, J.O., Xynogalas, M., Osayande, N., and Olotu, S. (2008) *Fluid discrimination and reservoir characterization from onshore Niger Delta. Annual General Meeting, Las Vegas, Society of Exploration Geophysicists*. 2001 – 2005.
- Pendrel, J. and Schouten, H. (2020) *Facies – The drivers for modern inversions. The Leading Edge*, **39**(2), 102 – 109.

- Samantaray, S. and Gupta, P. (2008) *An interpretative approach for gas zone identification and lithology discrimination using derivatives of  $\lambda^*p$  and  $\mu^*p$  attributes, 7th Biennial international Conference and Exposition on Petroleum Geophysics, —HYDERABAD 2008, Society of Petroleum Geophysicists, 386 - 341.*
- Short, K.C., and Stauble, A.J. (1967) *Outline of geology of Niger Delta. American Association of Petroleum Geologists, Bulletin* **51**(5), 761 – 799.
- Simm, R. and White, R.E. (2002) *Phase, polarity and the interpreter's wavelet, First Break* **20**(5), 277-281.
- Tuttle, M.L.W., Charpentier, R.R. and Brownfield, M.E. (1999) *The Niger Delta Petroleum System: Niger Delta Province, Nigeria, Cameroon, and Equatorial Guinea, Africa. USGS Science for a changing world, Open-File Report 99-50-H, 1-70.*
- Webb, B., Salerno, S., Rizzetto, C., Panizardi, J., Marchesini, M., Fervari, M., De Draganich, C., Colombi, N., and Calderoni, M. (2020) *A time-lapse case study in West Africa: Integrating disciplines for a complete reservoir study and field management. The Leading Edge*, **39**(2). 110 – 118.
- White, R. and Simm, R. (2003) *Tutorial: Good practice in well ties. First Break*, **21**(5), 75 – 83.
- White, R.E. (1997) *The accuracy of well ties: practical procedures and examples, Expanded Abstract RC1.5, 67th SEG Meeting, Dallas.*